J Supercond Nov Magn (2014) 27:2835–2839
DOI 10.1007/s10948-014-2770-2

ORIGINAL PAPER

Polyol Synthesis of Fe_3O_4@Tween20 Nanocomposite in Vaseline Oil

S. Esir · A. Baykal · H. Sözeri

Received: 26 August 2014 / Accepted: 1 September 2014 / Published online: 14 September 2014

Abstract For the synthesis of Fe_3O_4@Tween20 nanocomposite, two surfactants (Tween20 and oleic acid) were used to overcome the aggregation. The nanoparticles were used to prepare a water-based Fe_3O_4@Tween20 nanocomposite using oleic acid and Tween20 as surfactants (Fe_3O_4 colloidal superparticles were developed by introducing Tween20 as a surface modification agent to maintain the colloidal stability of the Fe_3O_4 superparamagnetic nanoparticles (SPION)). Vaseline and the synthesized iron oleate were used for the polyol synthesis of Fe_3O_4@Tween20 nanocomposite. The product has superparamagnetic property. Fourier transform infrared spectroscopy (FT-IR) and thermal gravimetric analysis (TGA) proved the presence of both surfactants on the surface of the Fe_3O_4 nanoparticles. The product may have potential use in magnetic resonance imaging and hyperthermia.

Keywords Fe_3O_4 · Ween20 · Anocomposite · Agnetic nanomaterials

1 Introduction

There has been a growing interest for coating the inorganic nanoparticles with conducting polymer to form core/shell-structured materials to enhance the stability of composites and widen the applications because of the strong electronic interaction between the inorganic core and polymer shell [1, 2].

To overcome the aggregation problem, the outer surface of the Fe_3O_4 superparamagnetic nanoparticles (SPION) is covered with deposit inert shell layers (polymeric or organic layer). SPIONs have considerable interest due to their potential applications in biotechnology, including magnetic resonance imaging (MRI) contrast enhancement, targeted drug delivery, and the separation and purification of biomolecules, biosensors [3–6].

Tween20 (TW20) is a polysorbate, nonionic surfactant substance, and such sorbitan ester ethoxylates (commercially known as Tween) are common nonionic surfactants which contain short poly(ethylene oxide) chains attached to sorbitol and have a low molecular weight [7–9]. Tween surfactants are extensively used in food, cosmetic, and pharmaceutical preparations, bioresearch, and chemical compound detection owing to their nontoxicity, emulsification, and other advantages [10–12]. Tween20 has better water solubility than other Tweens and therefore has drawn much attention.

In the present work, a low-cost and facile method is suggested to synthesize Fe_3O_4@Tween20 nanocomposite. Iron oleate was utilized as a ferrous resource in the thermal decomposition method, and Tween20 was employed as a surfactant to form the miniemulsion and stabilize the SPIONs in aqueous solutions. The low-cost mineral oil (Vaseline) was used as the solvent for the Fe_3O_4 nanoparticles (NPs) and the carrier of the magnetic fluid. Vaseline was chosen due to its high boiling point, good thermal stability, and low cost.

S. Esir · A. Baykal (✉)
Department of Chemistry, Fatih University, B. Cekmece, 34500 Istanbul, Turkey
e-mail: hbaykal@fatih.edu.tr

H. Sözeri
TUBITAK-UME, National Metrology Institute, PO Box 54, 41470 Gebze-Kocaeli, Turkey

2 Experimental

2.1 Chemicals and Materials

Ferric chloride ($FeCl_3.6H_2O$, 99 %), ethanol, oleic acid, NaOH, methanol, Vaseline oil, and Tween20 were purchased from Merck and used without any purification.

2.2 Instrumentations

X-ray powder diffraction (XRD) analysis was conducted on a Rigaku Smart Lab Diffractometer operated at 40 kV and 35 mA using Cu Kα radiation.

Transmission electron microscopy (TEM) analysis was performed using a FEI Tecnai G2 Sphera microscope. A drop of diluted sample in alcohol was dripped on a TEM grid.

Fourier transform infrared (FT-IR) spectra were recorded in transmission mode with a Perkin Elmer BX FT-IR infrared spectrometer. The powder samples were ground with KBr and compressed into a pellet. FT-IR spectra in the range of 4,000–400 cm^{-1} were recorded in order to investigate the nature of the chemical bonds formed.

VSM measurements were performed by using a vibrating sample magnetometer (LDJ Electronics Inc., Model 9600). The magnetization measurements were carried out in an external field up to 15 kOe at room temperature.

Thermal stability was determined by thermogravimetric analysis (TGA, Perkin Elmer Instruments model, STA 6000). The TGA thermograms were recorded for 5 mg of powder sample at a heating rate of 10 °C/min in the temperature range of 30–800 °C under synthetic air atmosphere.

2.3 Synthesis of Iron Oleate

The iron oleate complex were prepared by reaction oleic acid and Fe^{3+} chlorides. Ten millimoles of $FeCl_3.6H_2O$ was dissolved in 50 ml methanol under vigorous stirring. Then, 0.5 ml oleic acid was added into this solution; 30 mmol NaOH was dissolved in 100 ml methanol in another beaker, which was then poured into Fe^{3+} oleic acid mixture. The final mixture was refluxed at 200 °C for 3 h. The mixed iron oleate was obtained after drying at 80 °C.

2.4 Synthesis of Fe_3O_4@Tween20 Nanocomposite

Five grams of iron oleate complex, 100 ml Vaseline oil, and 5 g of Tween20 were mixed and magnetically stirred for 1 h under Ar atmosphere. The mixture was then heated to 350 °C with a heating rate of 10 °C/min and held at this temperature for 40 min under Ar gas with continuous stirring. Then the Fe_3O_4@Tween20 nanocomposite was separated magnetically and was washed three times with ethanol and water, respectively, to remove the remaining impurities (Scheme 1).

3 Results and Discussion

3.1 XRD Analysis

Phase investigation of the crystalline product was performed by XRD and the diffraction pattern is presented in Fig. 1. The XRD pattern indicates that the product consists of magnetite, Fe_3O_4, and the diffraction peaks are broadened owing to very small crystallite size. All of the observed diffraction peaks are indexed by the cubic structure of Fe_3O_4 (JCPDS no. 19-629), revealing a high-phase purity of magnetite. The mean size of the crystallites was estimated from the diffraction pattern by line profile fitting method using the (1) given in [13] and [14]. The line profile, shown in Fig. 1 was fitted for the observed five peaks with the following Miller indices: (220), (311), (400), (511), and (440). The average crystallite size, D and σ, was obtained as 10 ±4 nm as a result of this line profile fitting.

3.2 FT-IR Analysis

FT-IR spectra of oleic acid, Tween20, bulk Fe_3O_4, and Fe_3O_4@Tween20 are given in indicators a–d of Fig. 2, respectively. The presence of the iron oxide nanoparticles evidenced by the strong absorption bands at around

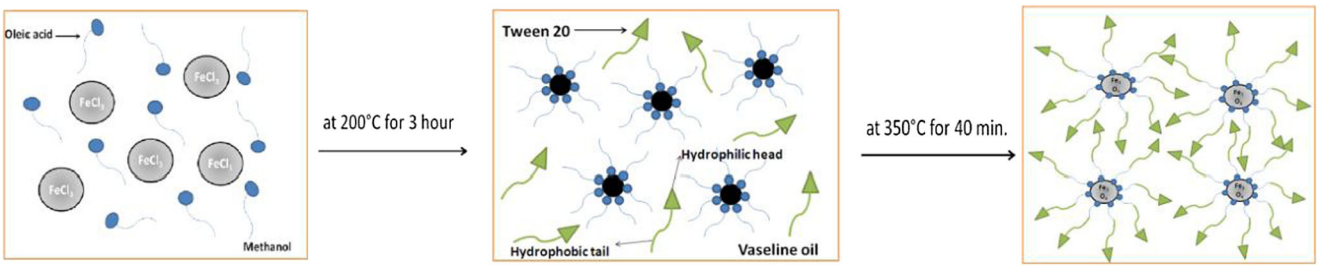

Scheme 1 Reaction scheme for the synthesis of Fe_3O_4@Tween20 nanocomposite

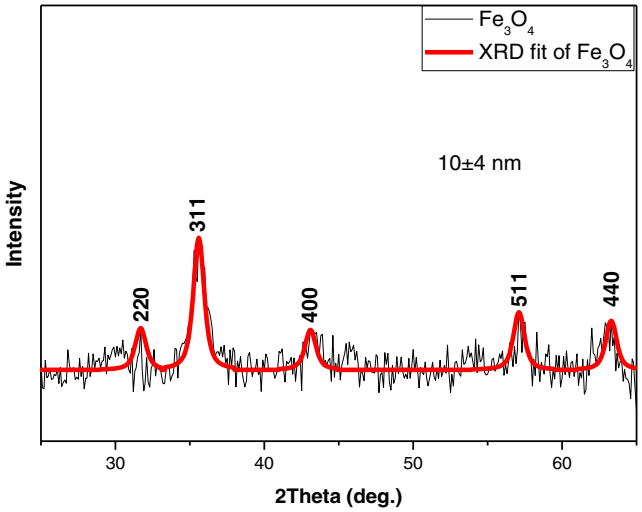

Fig. 1 XRD powder pattern of Fe_3O_4@Tween20 nanocompositeosite

570–590 cm^{-1} confirm that the metal-oxygen stretching (Fe–O bond) is present (Figs. 2c and d) [15–17]. The presence of surface organic groups is important for Fe_3O_4 NPs in stabilizing [18]. Two distinct peaks at 1,450 and 1,555 cm^{-1} were observed in case of capped samples corresponding to symmetric and asymmetric COO−−tretching vibrations, thereby confirming that OA is chemically bound to the surface of MN (Figs. 2a and b). The broad absorption peak at about 1,120 cm^{-1} could be ascribed to either linkage of Tween20 [19, 20]. The peaks at 3,840 and 2,910 cm^{-1} can be assigned to the stretching vibrations of CH_2 in the aliphatic chain of oleic acid and Tween20.

3.3 TG Analysis

TGA thermogram of Fe_3O_4@Tween20 nanocomposite is presented in Fig. 3, which can be used for a quantitative

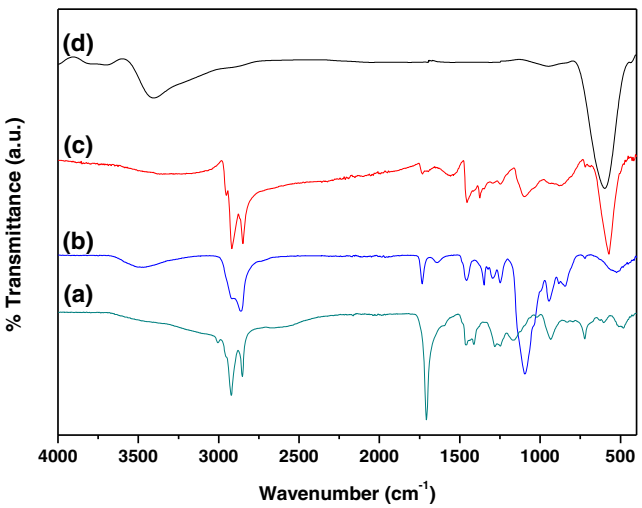

Fig. 2 FT-IR spectra of *a* oleic acid, *b* Tween20, *c* Fe_3O_4 magnetic fluid, and *d* bulk Fe_3O_4

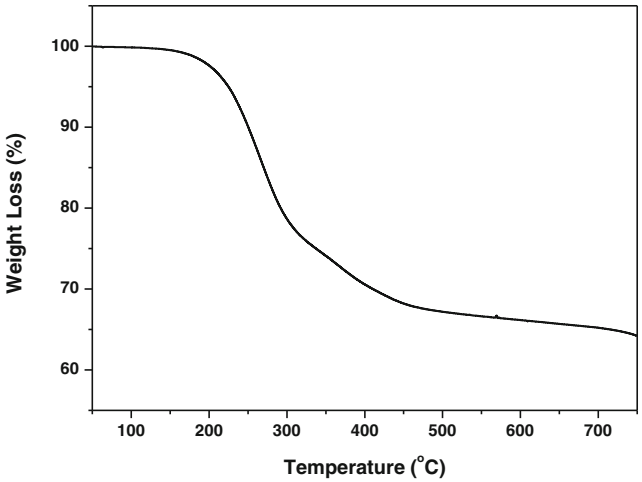

Fig. 3 Thermogram of Fe_3O_4@Tween20 nanocomposite

comparison of degradation behavior of different samples. Iron oxide shows no weight loss in the temperature range of TG analysis. On the other hand, degradation is seen in the TGA curves of both oleic acid and Tween20. Fe_3O_4@Tween20 nanocomposite shows a slight weight loss, while both oleic acid and Tween20 exhibit a considerable thermal stability up to 200 °C. Based on the thermogram, organic content (oleic acid and Tween20) is 35 %, which means an inorganic content (Fe_3O_4 NPs) is about 65 %.

3.4 TEM Analysis

Fe_3O_4@Tween20 nanocomposite was investigated by TEM, as shown in Fig. 4. Average particle size wascalculated by log-normal fitting to the size distribution histogram and was obtained as 19 ± 2 nm. It is clear that the particle size obtained from the XRD analysis is smaller than that observed from the TEM micrograph. The nanoparticles with slight aggregation may result in the difference in size between XRD and TEM analysis.

3.5 VSM Analysis

The room-temperature magnetic hysteresis curve of magnetic property of Fe_3O_4@Tween20 nanocomposite was presented in Fig. 5. As it can be seen from Fig. 5, the absence of remanence or coercivity indicates the superparamagnetic property of the product. The saturation magnetization (Ms calculated from a plot of Mvs. $1/H$(Mat $1/H \geq 0$)) value of experimental curve is calculated as 23.4 emu/g at room temperature which is also verified by the lognormal weighted Langevien fit of this curve. This value is comparatively lower than that of bulk magnetite with an Ms of 92 emu/g [21–24] and it is frequently observed in magnetic nanoparticles. This reduced

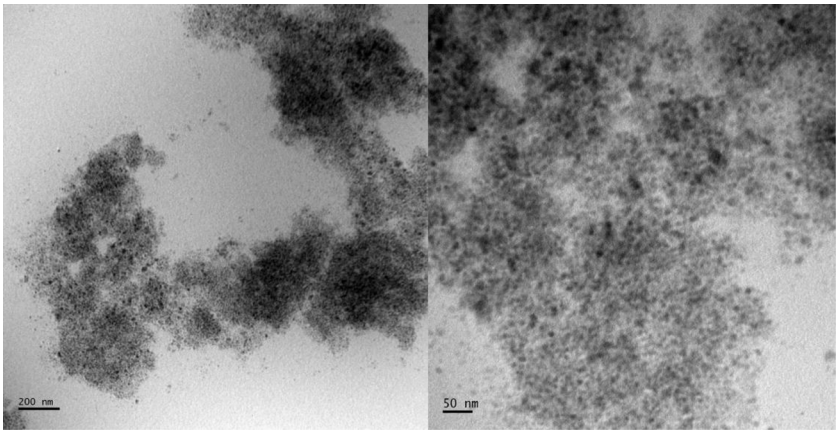

(a)

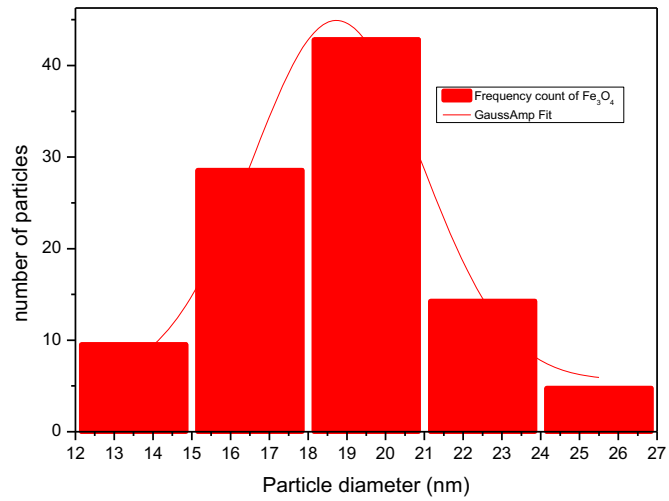

(b)

Fig. 4 **a** TEM micrographs and **b** particle size distribution diagram of Fe_3O_4@Tween20 nanocomposite

magnetization was explained by Kodama et al. via the presence of disordered spins on the surface of nanoparticles, which is known as spincanting effect [25] The lower saturation magnetization of the composite particles may be attributed to the diamagnetic contribution of the surfactant shells surrounding the magnetite nanoparticles [21].

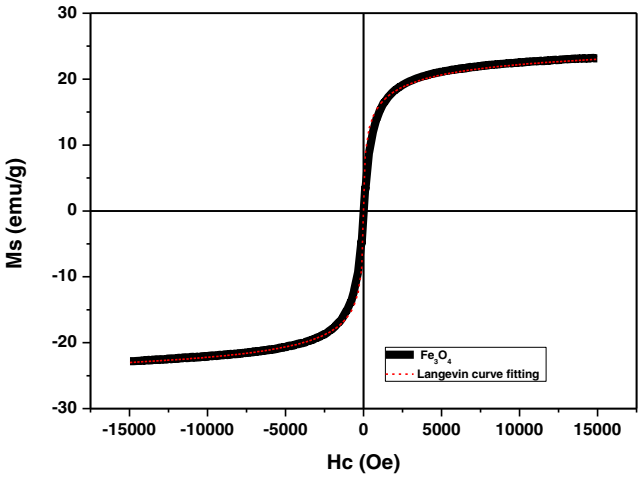

Fig. 5 Magnetic hysteresis curve of Fe_3O_4@Tween20 nanocomposite

The RT hysteresis curve is well fitted with the lognormal weighted Langevien function [26]:

$$M(H, D) = \sum M_i V_i f(d_i) L(x_i) \quad (1)$$

where M_i and V_i are magnetization and volume of ith particle, respectively, $f(d_i)$ is log-normal size distribution function, and $L(x_i)$ is the Langevien function. The details and calculation of the mean diameter of NP can be found in our previous study [26]. The calculated average diameter, D_m, of 16.5 nm was obtained by fitting curve. The magnetic core size obtained for iron oxide from the fitting is slightly smaller than the size obtained from TEM and X-ray line profile fitting due to the presence of magnetically dead layer on the nanoparticle surface. This also confirms nearly single crystalline character of iron oxide NPs.

4 Conclusion

Polyol method was sued for the synthesis of Fe_3O_4 @Tween20 nanocomposite. For this synthesis, iron oleate was synthesized via modified reflux method. As a reaction solvent, Vaseline was used instead of other expensive high-boiling-point solvent. Due to that, this is the first study in which Vaseline was used as a reaction solvent. Although the surface modification was done using both oleic acid and Tween20 to overcome the aggregation, slight aggregation was also observed. The crystallite, particle size, and magnetic core size are coinciding with each other. Controlled polyol synthesis of such Fe_3O_4@Tween20 nanocomposite may produce controllable nanoscale properties, and they may be used in MR contrast enhancement and hyperthermia.

Acknowledgments This work was supported by Fatih University under BAP Grant No. P50021301-Y (3146) and Turkish Research Council (Project No. 113F158).

References

1. Singh, K., Ohlan, A., Bakhshia, A.K., Dhawan, S.K.: Mater. Chem. Phys. **119**, 201 (2010)
2. Li, Y., Chen, G., Li, Q., Qiu, G., Liu, X.: J. Alloy Compd. **509**, 4104 (2011)
3. Jacintho, G.V.M., Brolo, A.G., Corio, P., Suarez, P.A.Z., Rubim, J.C.: J. Phys. Chem. C **113**, 7684 (2009)
4. Heinemann, A., Wiedenmann, A.: J. Magn. Magn. Mater. **289**, 149 (2005)
5. Jeong, U., Teng, X.W., Wang, Y., Yang, H., Xia, Y.N.: Adv. Mater. **19**, 33 (2007)
6. Zhao, Y.X., Zhuang, L., Shen, H., Zhang, W., Shao, Z.J.: J. Magn. Magn. Mater **321**, 377 (2009)
7. Zhang, H., Xu, G., Liu, T., Xu, L., Zhou, Y.: Colloids and Surfaces A: Physicochem. Eng. Asp. **416**, 23 (2013)
8. Balakrishnan, B., James, N.R., Jayakrishnan, A.: Polym. Int. **54**, 1304 (2005)
9. Dikici, A., Arslan, A., Yalcin, H., Ozdemir, P., Aydin, I., Calicioglu, M.: Food Control **30**, 365 (2013)
10. Dimitrova, T.D., Leal-Calderon, F.: Langmuir **15**, 8813 (1999)
11. Ruiz, C.C., Molina-Bolivar, J.A., Aguiar, J., MacIsaac, G., Moroze, S., Palepu, R.: Colloid Polym. Sci. **281**, 531 (2003)
12. Batteiger, B., Newhall, W.J.t., Jones, R.B.: J. Immunol. Methods **55**, 297–307 (1982)
13. Wejrzanowski, T., Pielaszek, R., Opalińska, A., Matysiak, H., Lojkowski, W., Kurzydlowski, K.J.: Appl. Surf. Sci. **253**, 204 (2006)
14. Pielaszek, R.: Applied Crystallography Proceedings of the XIX Conference, Krakow, Poland, p. 43 (2003)
15. Kirwan, L.J., Fawell, P.D., Bronswijk, W.V.: Langmuir **19**, 5802 (2003)
16. Durmus, Z.: Synthesis and Characterization Of Coated Magnetic Spinel Nanoparticles. Master Thesis, Fatih University Istanbul (2009)
17. Özkaya, T., Toprak, M.S., Baykal, A., Kavas, H., Köseoğlu, Y., Aktaş, B.: J. Alloys Compd. **472**, 18 (2009)
18. Bateer, B., Qu, Y., Tian, C., Du, S., Ren, Z., Wang, R., Pan, K., Fu, H.: Mater Res. Bull. **56**, 34 (2014)
19. Wang, Y.M., Cao, X., Liu, G.H., Hong, R.Y., Chen, Y.M., Chen, X.F., Li, H.Z., Xu, B., Wei, D.G.: J. Magn. Magn. Mater **323**, 2953 (2011)
20. Jadhav, N.V., Prasad, A.I., Kumar, A., Mishra, R., Dhara, S., Babu, K.R., Prajapat, C.L., Misra, L., Ningthoujam, R.S., Pandey, B.N., Vatsa, R.K.: Colloids Surf. B: Biointerfaces **108**, 158–168 (2013)
21. Lin, C.C., Ho, J.M.: Ceramics International **40**, 10275 (2014)
22. Han, D.H., Wang, J.P., Luo, H.L.: J. Magn. Magn. Mater **136**, 176 (1994)
23. Chikazumi, S.: Physics of Ferromagnetism, 2nd edn. Clarendon, Oxford (1997)
24. Blum, E., Cebers, A., Maiorov, M.M.: Magnetic Fluids. Walter de Gruyter, Berlin (1997)
25. Kodama, R.H., Berkowitz, A.E., McNiff, E.J., Foner, S.Jr.: Phys. Rev. Lett. **77**(2), 394 (1996)
26. Kavas, H., Baykal, A., Toprak, M.S., Koseoglu, Y., Sertkol, M., Aktas, B.: J. Alloy Compd. **479**, 49 (2009)